Effects of metal-doped indium-tin-oxide buffer layers in organic light-emitting devices

T.-H. Chen, T. J. Wu, J. Y. Chen, and Y. Liou

Citation: Journal of Applied Physics **99**, 114515 (2006); doi: 10.1063/1.2198932
View online: http://dx.doi.org/10.1063/1.2198932
View Table of Contents: http://scitation.aip.org/content/aip/journal/jap/99/11?ver=pdfcov
Published by the AIP Publishing

Effects of metal-doped indium-tin-oxide buffer layers in organic light-emitting devices

T.-H. Chen
ULVAC Taiwan Inc., Taipei, Taiwan and Display Institute, National Chiao Tung University, Hsinchu, Taiwan, Republic of China

T. J. Wu and J. Y. Chen
ULVAC Taiwan Inc., Taipei, Taiwan, Republic of China

Y. Liou[a)]
Institute of Physics, Academia Sinica, Taipei, Taiwan, Republic of China

(Received 20 July 2005; accepted 29 March 2006; published online 12 June 2006)

Organic light-emitting devices were fabricated by using different metal (V, Zr, Hf)-doped indium-tin-oxide (ITO) buffer layers on an ITO anode. The metal-doped ITO buffer layers were 15 nm thick with different metal concentrations. Both resistivity and work function of the ITO buffer layer were manipulated by these metal dopants. Different effects on the devices, such as reduced turn-on voltage, improved luminance, and enhanced current efficiency, were investigated. A low turn-on voltage was observed for devices with small work function and resistivity. The lowest turn-on voltage (3 V) was found on a device with a V-doped ITO buffer layer. The devices usually have a similar current density (J)-voltage (V) characteristics, but not the luminance-J or the current efficiency-J characteristics when the ITO buffer layers have the same work function. The devices with the Hf-doped ITO buffer layers show the best luminance performance among those considered. At 100 mA/cm^2, a luminance of 15,000 cd/m^2, and a current efficiency of 15 cd/A have been achieved. The balance between the carrier concentration and the energy barrier for the hole injection is possibly responsible for such performance. © *2006 American Institute of Physics*.
[DOI: 10.1063/1.2198932]

I. INTRODUCTION

Organic light emitting devices (OLEDs) have already been recognized as potential future major flat panel displays due to their high brightness, high efficiency, full color, and low operating voltage. Highly transparent and conducting indium-tin-oxide (ITO) films have been the most commonly used anode in optoelectronic devices and OLEDs.[1–5] A typical OLED consists of an ITO anode followed by a hole transport layer (HTL) [N,N′-bis-(1-naphthyl)-N,N′-diphenyl1-1,1-biphenyl 1-4,4′-diamine (NPB)], a light emissive layer, together with an electron transport layer (ETL) [tris(8-hydroxyquinoline) aluminum (Alq_3)], and a metal cathode [Mg:Ag]. Charge injection from the electrodes to the organic materials plays an important role in the device performance. Band alignment between each organic layer and the electrodes is crucial for reducing the energy barrier; for example, the highest occupied molecular orbital (HOMO) of NPB is 5.7 eV matches the HOMO of Alq_3 (5.9 eV). To avoid large energy differences between the ITO anode and the NPB, a buffer layer with a work function (or ionization potential [IP]) between the ITO anode and the HOMO of the NPB has been employed. Usually, the mobility of holes in the HTL is much higher than that of the electrons in the ETL used in OLEDs. Reducing the number of holes in the HTL or enhancing electron injection in the ETL helps to improve electron-hole current balance in OLEDs. It is common to modify the two electrodes in order to balance the current in OLEDs. The hole injection at the anode can be adjusted by using different surface treatments as well as by inserting a buffer layer between the ITO and the HTL.[6–10] It is well known that a thin layer of copper phthalocyanine (CuPc) with an IP of about 5.2 eV on the ITO anode can dramatically enhance the device stability and performance by reducing the effective barrier between the ITO and the HTL.[11–13] However, it was also reported that a CuPc buffer layer will decrease the hole injection efficiency, which leads to the balance of charge (hole and electron) injection and recombination.[14] Such a contradiction has been found in other materials used in OLEDs. Various oxide (SiO_2, transition metal oxides, etc.) buffer layers on an ITO anode have demonstrated their capabilities of lowering the

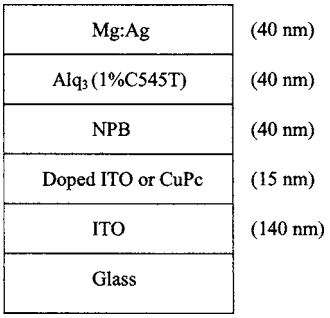

FIG. 1. OLED device structure.

[a)]Author to whom correspondence should be addressed; electronic mail: yung@phys.sinica.edu.tw

TABLE I. The dopants, concentrations, resistivities and work functions of each device are listed.

Name	Doped elements	Concentractions (mol. %)	Resistivity (Ω-cm)	Work function (eV)
V1	Vanadium	6	10	5.0
V2	Vanadium	10.5	500	5.2
V3	Vanadium	12.5	10,000	5.4
Zr1	Zirconium	5	10	5.0
Zr2	Zirconium	8	2,000	5.4
Hf1	Hafnium	2	2	5.0
Hf2	Hafnium	4	10	5.2
Hf3	Hafnium	10	10,000	5.4

turn-on voltage, enhancing the luminance efficiency, and extending lifetime of OLEDs.[15–20] The device performance enhancement has been attributed to the increased work function, the reduced energy barrier between the ITO anode and the HTL, and the enhanced hole injection. For thin (~2 nm) oxide layers, the tunneling mechanism was proposed and the barrier reduction was attributed to the band bending mechanism.[21] However, a balance of the charge injection may have been achieved due to the increasing contact resistance from the insulating oxide buffer layer between the ITO anode and the HTL. The hole accumulation and the hole injection suppression from the anode to the HTL may be concluded from the rising of contact resistance. The space-charge buildup due to the hole accumulation may lead to the space-charge-limited hole injection, which can be determined from the *J-V* characteristics. In our previous reports, we have shown that the balance of the carrier concentration and the energy barriers for the hole injection was significant to the device performance enhancement.[22,23]

In this report, we have conducted an experiment by doping different metals (V, Zr, Hf) into the ITO as a buffer layer which resulted in different work functions and resistivities. Since the resistivity versus temperature properties of these metals have the characteristics of semiconductors for all metal-doped ITO films, their resistivity is related to the carrier densities. It is confirmed by the electron spectroscopy for chemical analysis (ESCA) method that most of the doped metals in the ITO layer have transformed into metal-oxides (MO_x). The uniformly doped MO_x in the ITO layer has increased the work function and the resistivity by reducing the oxygen deficiency.

With the additional 15 nm thick metal-doped ITO layer, there was no significant change (<2%) on the transparency of the whole ITO film (155 nm thick). A green coumarin derivative, 10-(2-benzothiazolyl)-1,1,7,7-tetramethyl-2,3,6,7 - tetrahydro - 1H,5H,11H - benzo [l] pyrano [6,7,8-ij]

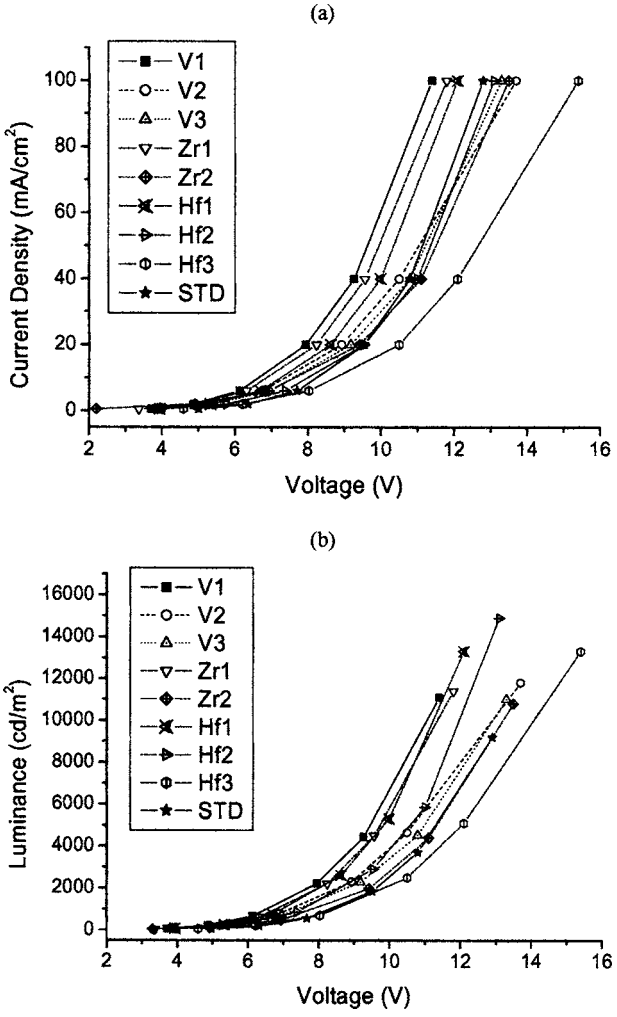

FIG. 2. J-V and L-V of all devices.

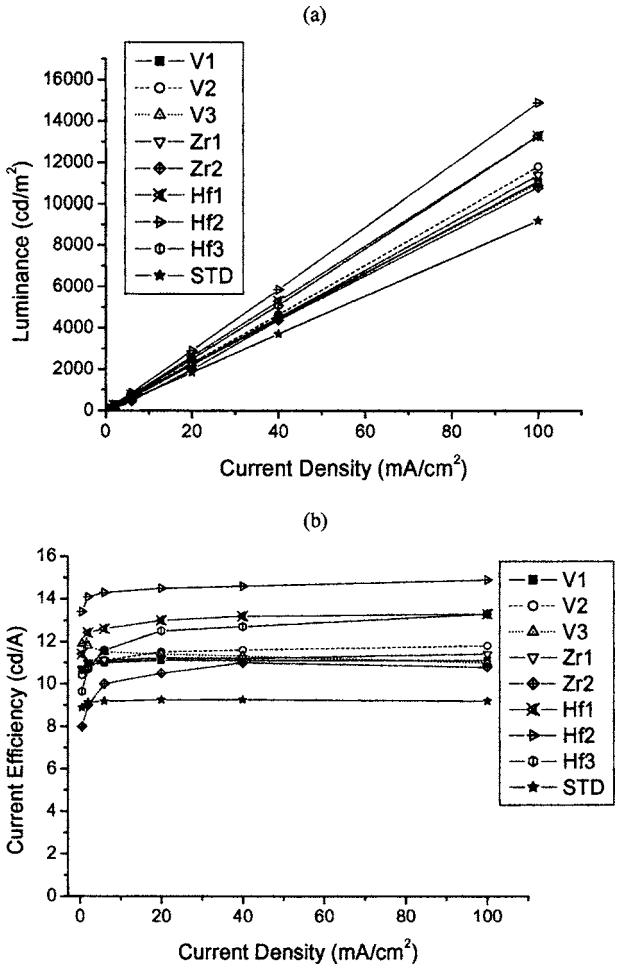

FIG. 3. L-J and current efficiency-J of all devices.

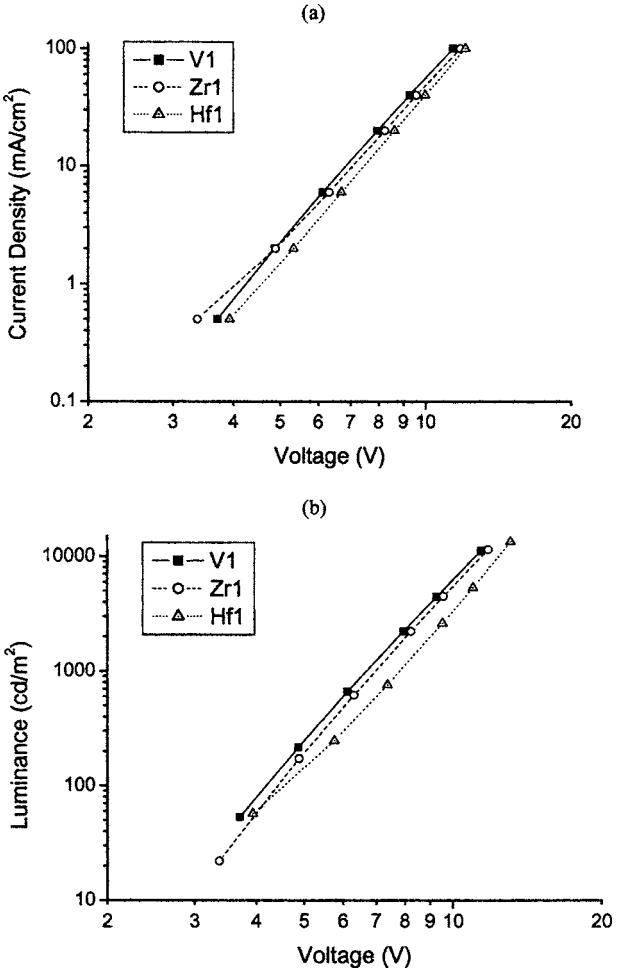

FIG. 4. J-V and L-V of V1-, Zr1- and Hf1-doped devices.

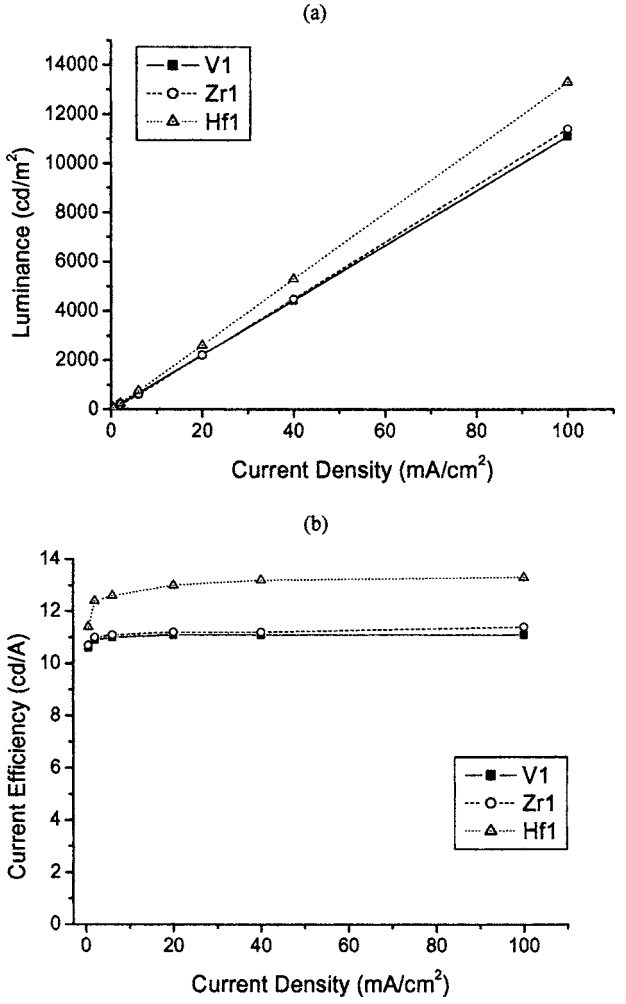

FIG. 5. L-J and current efficiency-J of V1-, Zr1- and Hf1-doped devices.

quinolizin-11-one (C-545T), was doped in the light emissive layer (Alq_3) due to its thermal stability and electroluminescence (EL) performance.[24] To compare and understand the significance of the device performance between the doped and undoped emissive layer, readers have to check with other previously published reports.[25]

II. EXPERIMENT

ITO films of 140 nm thick and the extra metal-doped ITO layers (15 nm) were deposited on glass substrates by using a RF (for ITO) and dc (for metal) cosputtering system. The ITO target is composed of In_2O_3:SnO_2 (9:1), and the metal (V, Zr, Hf) targets are 99.9% pure. The base pressure in the system was approximately 1.0×10^{-6} Torr. The system pressure was about 5 mTorr during the film deposition. By controlling the gas flow rate, a gas mixture of about 8% of oxygen in argon was achieved. The substrate temperature was kept at 300 °C. To control the metal contents in ITO, we changed the sputtering rate of each target. The chemical information of each element in the film was characterized by the electron spectroscopy for chemical analysis (ESCA). The concentrations of V in ITO have been determined by both the Rutherford backscattering (RBS) and the secondary ion mass spectrometry (SIMS) depth profile. We have observed a constant metal concentration in the doped ITO layer (15 nm) and a sharply decayed metal profile (<20 nm) in the undoped ITO film. The transmittance of the metal-doped ITO (150 Å)/ITO (1400 Å) film was about 90% (at 550 nm). After the ITO (140 nm) film and the metal-doped ITO layer (15 nm) are deposited, all organic layers—NPB (40 nm), Alq_3 (40 nm) (doped with C545T)—were deposited consecutively in vacuum by thermal evaporation with base pressure less than 10^{-7} Torr. After the deposition of the organic layers without a vacuum break, the Mg:Ag (10:1, 40 nm) and Ag (100 nm) for protection were deposited on top of the organic layers with separated deposition sources. For comparison, we have used a standard device (STD) with a 15 nm thick layer of CuPc on top of the ITO film (140 nm) without the metal-doped ITO layer by thermal evaporation during the device fabrication. The active area of the device was about 0.1 cm^2. These devices were completed with encapsulation in a dry argon glove box. The EL emission spectra and current-voltage-luminance characteristics were measured with a diode array rapid scan system using a Photo Research PR650 spectrophotometer and a computer-controlled dc source.

III. RESULTS AND DISCUSSION

We have used different transition metals (V, Zr, and Hf) to dope ITO films as buffer layers between the ITO anode

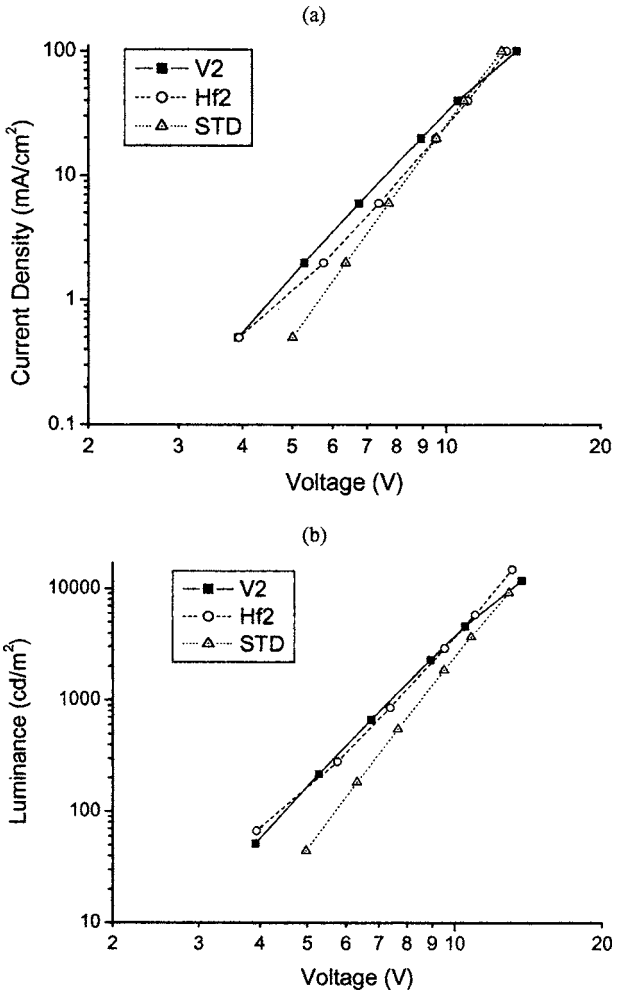

FIG. 6. J-V and L-V of V2-, Hf2-doped and standard devices.

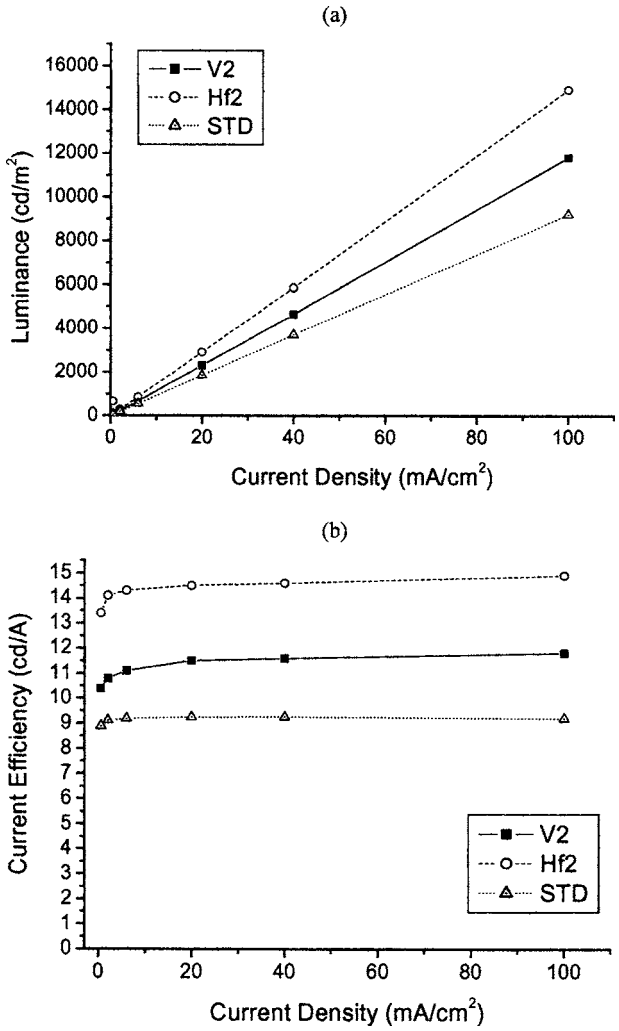

FIG. 7. L-J and current efficiency-J of V2-, Hf2-doped and standard devices.

and the HTL (NPB) to fabricate the EL devices. The device structure is shown in Fig. 1. The experiment was conducted by doping ITO films with different concentrations of metals in order to obtain desired work functions (5, 5.2, and 5.4 eV). Since these metals were oxidized in the film quickly, it is expected that the resistivity was dependent on the concentration of the metal dopants. From both the RBS and ESCA analyses, the oxygen concentrations in the metal-doped ITO films were increased from about 10% to 17% compared to the nondoped ITO film. The oxide formation or the reduction of the oxygen deficiency resulted in the increment of the work function and the resistivity. In Table I, we listed the properties of different metal-doped ITO films. The current density (J)-voltage (V) and the luminance (L) vs V characteristics of these devices are shown in Fig. 2. The device with V1-doped ITO layer shows the best J-V and L-Vcharacteristics, as shown in Fig. 2. The luminance (L) versus current density (L-J) and current efficiency versus J characteristics are shown in Fig. 3. The device with a Hf2-doped ITO layer shows higher L and current efficiency performances. It is shown that the characteristics of other devices are between the device with Hf2-doped ITO layer and the standard device. Since devices with V1, Zr1, and Hf1-doped ITO layers are similar in both J-V and L-V due to their similar work functions (~5 eV) and relatively low resistivities (10 ohm cm for V1-doped ITO, 10 ohm-cm for Zr1-doped ITO and 2 ohm cm for Hf1-doped ITO), further discussion will be made in Sec. III A. In Sec. III B, we'll discuss the devices with the V2, Hf2-doped ITO layers and the standard device due to their similar work functions, ~5.2 eV, but rather different resistivities: (10 ohm cm for Hf2-doped ITO, 500 ohm cm for V2-doped ITO, beyond measurement for standard sample). In Sec. III C, we'll discuss the devices with V3, Zr2, and Hf3-doped ITO layers since they have a similar work function (~5.4 eV), yet relatively high resistivities (10 000 ohm cm for V3-doped ITO, 2000 ohm cm for Zr2-doped ITO, and 10 000 ohm cm for Hf3-doped ITO).

A. Devices with 5 eV work functions and small resistivity

These devices have similar work functions (~5 eV) and relatively low resistivities; hence their characteristic curves are closed to each other. From the double-logarithmic plot [Fig. 4(a)], one can see the current density obeys a power law $J\alpha V^{m+1}$ with $m+1 \sim 2.5$. This behavior can be taken as an indication for the space-charge-limited conduction (SCLC). The carrier concentration is the dominant factor for

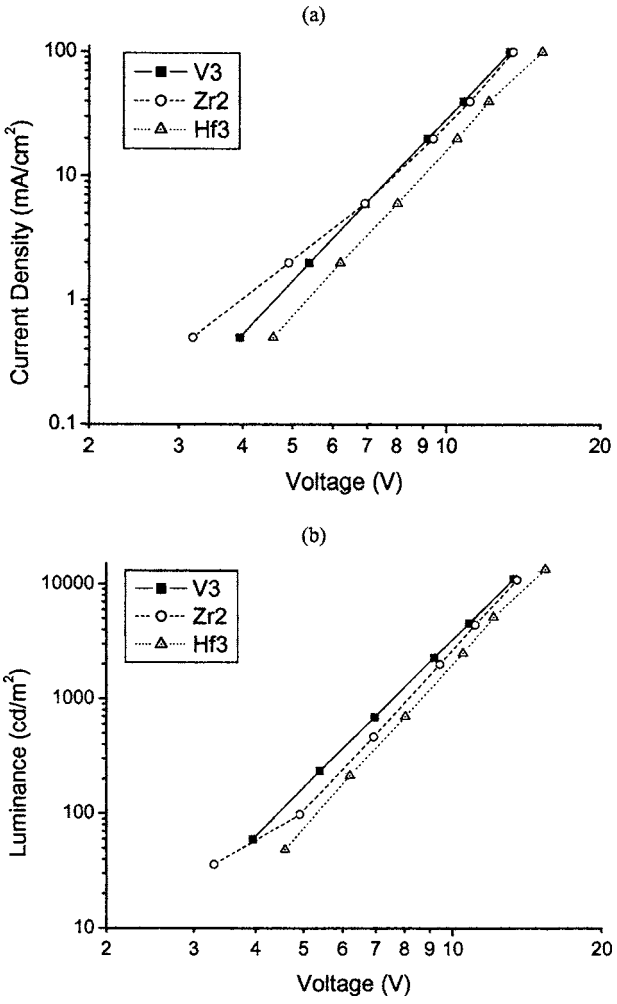

FIG. 8. J-V and L-V of V3-, Zr2- and Hf3-doped devices.

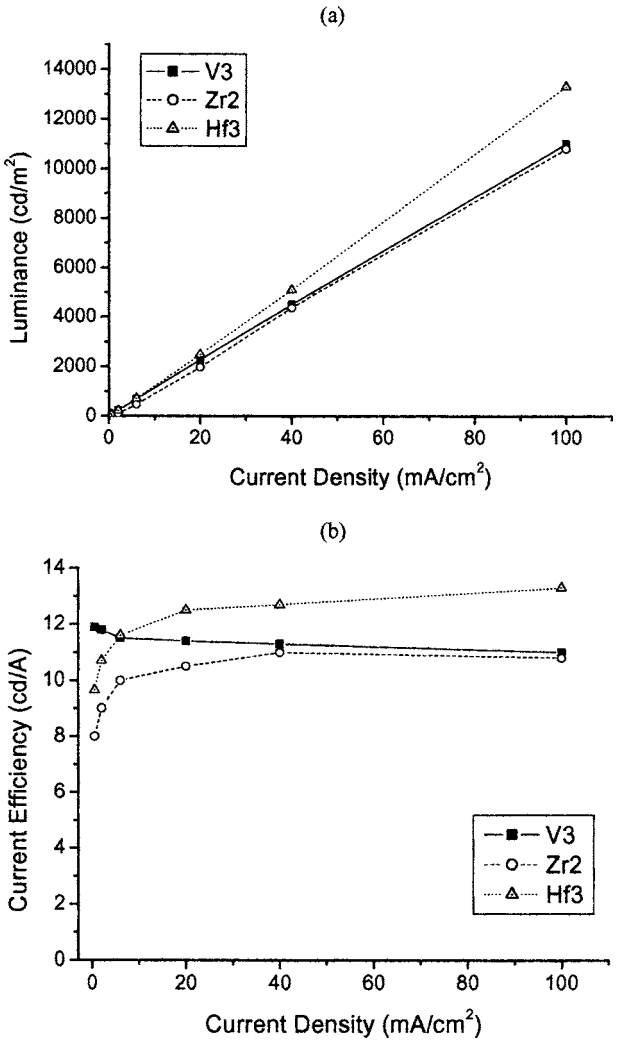

FIG. 9. L-J and current efficiency-J of V3-, Zr2- and Hf3-doped devices.

the device performance and it is much more important than the energy barrier for the hole injection. The device with the Hf1-doped ITO layer has the lowest resistivity (2 ohm cm) among three devices, its *L-V* curve also shows the difference, as shown in Fig. 4(b). In Fig. 5(a), the device with the Hf1-doped ITO layer has a relatively higher luminance in the *L-J* curves. From the current efficiency-*J* curves, as shown in Fig. 5(b), it's also clear that the device with the Hf1-doped ITO layer has a higher current efficiency. The good performance of the device with the Hf1-doped ITO layer may be attributed to its low doping concentration and resistivity. Although they have a similar energy barrier (work function) for hole injection, the device with the Hf1-doped ITO layer has the highest carrier concentration, which may enhance the *L* and the current efficiency.

B. Devices with 5.2 eV work functions and various resistivities

These devices have similar work functions (~5.2 eV) but significant differences in resistivity. The different characteristics are clearly shown in both *J-V* and *L-V* curves in Fig. 6. In Fig. 6(a), the Hf2 curve is nonlinear, which is quite different from the other two. The large slope of the standard device can be understood by its high resistivity. The large differences on their carrier concentrations lead to completely different characteristics in both *L-J* and the current efficiency-*J* curves, as shown in Fig. 7. The device with the Hf2-doped ITO layer has the best performances among them. It shows that the high carrier concentration is much more important than the energy barrier for the hole injection in these devices.

C. Devices with 5.4 eV work functions and relatively large resistivities

These devices have similar large work functions (~5.4 eV) and relatively large resistivities (>2 K ohm cm). The linearity with almost the same slope in the *J-V* and *L-V* curves is shown in Fig. 8. Since they all have large resistivities, their carrier concentrations must be low. The *L-J* and the current efficiency-*J* curves were similar for devices with V3- and Zr3-doped ITO layer, but not for the device with H3-doped ITO layer, as shown in Fig. 9. The device with the Hf3-doped ITO has the highest luminance and current efficiency, although it has a similar work function and resistivity. The exact reason is unclear, but it may be attributed to the dielectric property of the hafnium oxide in the Hf-doped ITO layer since all devices with the Hf-doped ITO layer have better performances than the others.

IV. CONCLUSION

We have compared the performance of OLEDs with different metal-doped ITO buffer layers. The resistivities and the work functions of the metal-doped ITO layer were dependent on the concentrations of the doped metals. While the metal-doped ITO layers have lower work functions and resistivities, the devices usually have lower turn-on and operating voltages as well. The device with the V1 (6%V)-doped ITO layer (work function 5 eV, resistivity 10 ohm cm) has achieved a turn-on voltage below 3 V, an operating voltage below 7 V (at 10 mA/cm^2), and a luminance of 1000 cd/m^2 below 7 V. Though the metal-doped ITO layers have the same work function, the devices may have similar characteristics on the *J-V* curves, yet different on the *L-J* curves or the current efficiency-*J* curves. The devices with the Hf2 (4%Hf)-doped ITO buffer layers show the highest luminance and current efficiency among all. At 100 mA/cm^2, a luminance of 15,000 cd/m^2, and a current efficiency of 15 cd/A have been achieved. The balance between the carrier concentration and the energy barrier for the hole injection is possibly responsible for such performance.

[1]C. W. Tang and S. A. VanSlyke, Appl. Phys. Lett. **51**, 913 (1987).
[2]C. Adachi, T. Tsutsui, and S. Saito, Appl. Phys. Lett. **55**, 1489 (1989).
[3]C. W. Tang, S. A. VanSlyke, and C. H. Chen, J. Appl. Phys. **85**, 3610 (1989).
[4]R. H. Friend, R. W. Gymer, A. B. Holmes, J. H. Burroughes, R. N. Marks, C. Taliani, D. D. C. Bradley, D. A. Dos Santos, J. L. Bredas, M. Logdlund, and W. R. Salaneck, Nature **397**, 121 (1999).
[5]J. Shi and C. W. Tang, Appl. Phys. Lett. **70**, 1665 (1997).
[6]C. Ganzorig, K.-J. Kwak, K. Yagi, and M. Fujihira, Appl. Phys. Lett. **79**, 272 (2001).
[7]H. Y. Yu, X. D. Feng, D. Grozea, Z. H. Lu, R. N. Sodhi, A.-M. Hor, and H. Aziz, Appl. Phys. Lett. **78**, 2595 (2001).
[8]W. Hu and M. Matsumura, Appl. Phys. Lett. **81**, 806 (2002).
[9]W. H. Kim, A. J. Makinen, N. Nikolov, R. Shashidhar, H. Kim, and Z. H. Kafafi, Appl. Phys. Lett. **80**, 3844 (2002).
[10]B. Low, F. Zhu, K. Zhang, and S. Chua, Appl. Phys. Lett. **80**, 4659 (2002).
[11]S. A. VanSlyke, C. H. Chen, and C. W. Tang, Appl. Phys. Lett. **69**, 2160 (1996).
[12]S. C. Kim, G. B. Lee, M.-W. Choi, Y. Roh, C. N. Wang, K. Jeong, J.-G. Lee, and S. Kim, Appl. Phys. Lett. **78**, 1445 (2001).
[13]E. W. Forsythe, M. A. Abkowitz, Y. Gao, and C. W. Tang, J. Vac. Sci. Technol. A **18**, 1869 (2000).
[14]S. M. Tadayyon, H. M. Grandin, K. Griffiths, P. R. Norton, H. Aziz, and Z. D. Popovic, Org. Electron. **5**, 157 (2004).
[15]C. O. Poon, F. L. Wong, S. W. Tong, R. Q. Zhang, C. S. Lee, and S. T. Lee, Appl. Phys. Lett. **83**, 1038 (2003).
[16]S. Y. Kim, J.-L. Lee, K.-B. Kim, and Y.-H. Tak, Appl. Phys. Lett. **86**, 133504 (2005).
[17]S. T. Lee, Z. Q. Gao, and M. R. Willis, Appl. Phys. Lett. **75**, 1404 (1999).
[18]Y. Shen, D. B. Jacobs, G. G. Malliaras, G. Koley, M. G. Spencer, and A. Ioannodis, Adv. Mater. (Weinheim, Ger.) **13**, 1234 (2001).
[19]C. Qiu, H. Chen, Z. Xie, M. Wong, and H. S. Kwok, Appl. Phys. Lett. **80**, 3485 (2002).
[20]C.-M. Hsu and W.-T. Wu, Appl. Phys. Lett. **85**, 840 (2004).
[21]K. H. Ho, J.-S. Kim, J. H. Burroughes, H. Becker, S. F. Y. Li, T. M. Brown, F. Cacialli, and R. H. Friend, Nature (London) **404**, 481 (2000).
[22]T. H. Chen, Y. Liou, T. J. Wu, and J. Y. Chen, Appl. Phys. Lett. **85**, 2092 (2004).
[23]T. H. Chen, Y. Liou, T. J. Wu, and J. Y. Chen, Appl. Phys. Lett. **87**, 243510 (2005).
[24]H. Kim, J. S. Horwitz, W. H. Kim, S. B. Qadri, and Z. H. Kafari, Appl. Phys. Lett. **83**, 3809 (2003).
[25]C. Chen and C. W. Tang, Appl. Phys. Lett. **79**, 3711 (2001).